March 2004

The NAD(P)H oxidase homolog Nox4 modulates insulin-stimulated generation of H_20_2 and plays an integral role in insulin signal transduction

Kalyankar Mahadev
Thomas Jefferson University

Hiroyuki Motoshima
Thomas Jefferson University

Xiangdong Wu
Thomas Jefferson University

Jean Marie Ruddy
Thomas Jefferson University

Rebecca S. Arnold
Emory University

See next page for additional authors

Authors
Kalyankar Mahadev, Hiroyuki Motoshima, Xiangdong Wu, Jean Marie Ruddy, Rebecca S. Arnold, Guangjie Cheng, J. David Lambeth, and Barry J. Goldstein

MOLECULAR AND CELLULAR BIOLOGY, Mar. 2004, p. 1844–1854 Vol. 24, No. 5
0270-7306/04/$08.00+0 DOI: 10.1128/MCB.24.5.1844–1854.2004

The NAD(P)H Oxidase Homolog Nox4 Modulates Insulin-Stimulated Generation of H_2O_2 and Plays an Integral Role in Insulin Signal Transduction

Kalyankar Mahadev,[1] Hiroyuki Motoshima,[1] Xiangdong Wu,[1] Jean Marie Ruddy,[1] Rebecca S. Arnold,[2] Guangjie Cheng,[2] J. David Lambeth,[2] and Barry J. Goldstein[1]*

Dorrance H. Hamilton Research Laboratories, Division of Endocrinology, Diabetes and Metabolic Diseases, Department of Medicine, Jefferson Medical College, Thomas Jefferson University, Philadelphia, Pennsylvania 19107,[1] and Department of Pathology and Laboratory Medicine, Emory University School of Medicine, Atlanta, Georgia 30322[2]

Received 3 September 2003/Returned for modification 8 October 2003/Accepted 26 November 2003

Insulin stimulation of target cells elicits a burst of H_2O_2 that enhances tyrosine phosphorylation of the insulin receptor and its cellular substrate proteins as well as distal signaling events in the insulin action cascade. The molecular mechanism coupling the insulin receptor with the cellular oxidant-generating apparatus has not been elucidated. Using reverse transcription-PCR and Northern blot analyses, we found that Nox4, a homolog of gp91*phox*, the phagocytic NAD(P)H oxidase catalytic subunit, is prominently expressed in insulin-sensitive adipose cells. Adenovirus-mediated expression of Nox4 deletion constructs lacking NAD(P)H or FAD/NAD(P)H cofactor binding domains acted in a dominant-negative fashion in differentiated 3T3-L1 adipocytes and attenuated insulin-stimulated H_2O_2 generation, insulin receptor (IR) and IRS-1 tyrosine phosphorylation, activation of downstream serine kinases, and glucose uptake. Transfection of specific small interfering RNA oligonucleotides reduced Nox4 protein abundance and also inhibited the insulin signaling cascade. Overexpression of Nox4 also significantly reversed the inhibition of insulin-stimulated IR tyrosine phosphorylation induced by coexpression of PTP1B by inhibiting PTP1B catalytic activity. These data suggest that Nox4 provides a novel link between the IR and the generation of cellular reactive oxygen species that enhance insulin signal transduction, at least in part via the oxidative inhibition of cellular protein-tyrosine phosphatases (PTPases), including PTP1B, a PTPase that has been previously implicated in the regulation of insulin action.

The elaboration of a large amount of cellular reactive oxygen species by hematopoietic phagocytic cells is essential for host defenses in bactericidal killing (1). However, more recently it has been appreciated that low levels of cellular oxidants, including superoxide and H_2O_2, are produced in a rapid temporal response to cellular growth factor and cytokine stimulation and are integral to the regulation of a variety of intracellular signaling pathways (41). Cellular reactive oxygen species have been shown to be elaborated in response to epidermal growth factor, platelet-derived growth factor, transforming growth factor β, and other growth factors (2, 3, 22, 37, 41) as well as with insulin stimulation (29, 34, 35).

Insulin signaling is initiated by the phosphorylation of specific tyrosyl residues of the cell surface insulin receptor, which activates its exogenous kinase activity and promotes the phosphorylation of IRS proteins on specific tyrosine residues (42). Much of insulin's downstream signaling to metabolic events involves the activation of phosphatidylinositol (PI) 3′-kinase activity by the docking of its p85 subunit to tyrosine-phosphorylated IRS-1 and IRS-2, which is linked to a network of distal signaling responses, including activation of protein kinase Akt and the stimulation of glucose uptake and other metabolic responses in specific cell types (23, 45). In parallel, insulin also activates cellular growth pathways mediated by Erk mitogen-activated protein kinases (MAPKs). In addition to these signaling events, our investigators have recently demonstrated that insulin stimulation of adipose and hepatoma cells leads to the rapid generation of cellular reactive oxygen species that facilitates both early and distal signal transduction through the insulin action pathway (34, 35). The effect of insulin-stimulated oxidant species is mediated at least in part via the oxidative inhibition of cellular protein-tyrosine phosphatases (PTPases), which depend on a reduced thiol moiety for catalytic activity and are normally inhibitory to insulin signal transduction (19, 37). PTP1B, in particular, has been considered to be a major candidate PTPase for the regulation of insulin action in a variety of studies, including knockout mouse models (13, 18, 25).

The molecular components of the insulin-responsive oxidant-generating activity in cell types that are targets for insulin action have not been identified. Previous work has demonstrated that the catalytic activity of the insulin-responsive system has enzymatic characteristics consistent with an NAD(P)H oxidase activity, catalyzing the reduction of molecular oxygen to generate superoxide, which undergoes subsequent dismuta-

* Corresponding author. Mailing address: Division of Endocrinology and Metabolic Diseases, Department of Medicine, Jefferson Medical College, Jefferson Alumni Hall, Suite 349, 1020 Locust St., Philadelphia, PA 19107-6799. Phone: (215) 503-1272. Fax: (215) 923-7932. E-mail: Barry.Goldstein@jefferson.edu.

tion to generate H_2O_2 (26–28, 38). The prototypic NAD(P)H oxidase complex from phagocytic cells has been extensively characterized. It consists of six subunits, including two plasma membrane-associated proteins, gp91*phox* and p22*phox*, which comprise flavocytochrome b_{558}, and four cytosolic factors, p47*phox*, p67*phox*, p40*phox*, and rac (1). The catalytic gp91*phox* subunit (also now known as Nox2) contains C-terminal homology to known flavoprotein dehydrogenases and consensus sequences comprising a putative NAD(P)H binding site (9, 39). Nox2 has recently been used in cloning studies to identify a small family of five homologous Nox [NAD(P)H oxidase] enzymes which are variably expressed in different tissues (8, 30).

To initiate studies into the molecular mechanism of the insulin-induced oxidant species in insulin-sensitive cells, in the present work we first identified that Nox4 was a prominent NAD(P)H oxidase catalytic subunit homolog expressed in adipose cells. Overexpression of wild-type Nox4 and Nox4 constructs lacking cofactor binding domains for NAD(P)H or FAD/NAD(P)H using adenovirus-mediated gene delivery in differentiated 3T3-L1 adipocytes revealed that the deletion constructs function as dominant negatives and suppress insulin-induced cellular oxidant generation and insulin signaling, including tyrosine phosphorylation of the insulin receptor and its substrate protein IRS-1, and attenuate the activation of downstream signaling kinases as well as glucose uptake. In parallel studies, reduction of Nox4 protein mass by transfection of specific small interfering RNA (siRNA) constructs also resulted in inhibition of the insulin action cascade. Overexpression of Nox4 also significantly reversed the inhibition of insulin-stimulated insulin receptor tyrosine phosphorylation induced by coexpression of PTP1B by inhibiting the catalytic activity of PTP1B. These data suggest that Nox4 provides a novel link between the insulin receptor and the generation of cellular reactive oxygen species that enhance insulin signal transduction via the oxidative inhibition of cellular PTPases, including PTP1B.

MATERIALS AND METHODS

Materials. Cell culture media and reagents were from Invitrogen (Carlsbad, Calif.); serum was from HyClone (Logan, Utah). 3T3-L1 cells were originally obtained from the American Type Culture Collection (Rockville, Md.). Human simian virus 40 (SV40)-transformed microvascular endothelial (HADMEC-5) cells (16) were a gift from John Flynn (Thomas Jefferson University). Human subcutaneous and omental adipose tissues were obtained at surgery with proper consent and procedures in accordance with the Institutional Review Board of Thomas Jefferson University. siRNAs were purchased from Dharmacon (Lafayette, Colo.). The Adeno-X expression system and rapid titer kit were from BD Biosciences (Palo Alto, Calif.). Recombinant human insulin was obtained from Sigma (St. Louis, Mo.). 5,6-Chloromethyl-2,7-dichlorodihydrofluorescein diacetate (CM-DCF-DA) was from Molecular Probes (Eugene, Oreg.); enhanced chemiluminescence (ECL) reagents were from NEN Life Science Products (Boston, Mass.). Monoclonal antiphosphotyrosine (4G10) and polyclonal antibodies to the insulin receptor β-subunit, IRS-1, and the p85 subunit of PI 3′-kinase were from Upstate Biotechnology (Lake Placid, N.Y.). Antibodies to phosphorylated Akt (Ser473) and Akt protein (not isoform specific) and phospho-Erk1/2 MAPK were from New England Biolabs (Beverly, Mass.). A monoclonal antibody to PTP1B (Ab-2) was obtained from Oncogene Research Products (San Diego, Calif.). Tris-acryl protein G was from Pierce (Rockford, Ill.). Horseradish peroxidase-conjugated secondary anti-mouse and anti-rabbit immunoglobulin G antibodies were obtained from Amersham Pharmacia Biotech (Piscataway, N.J.). 2-deoxy-D-[^{3}H]glucose was purchased from ICN (Costa Mesa, Calif.). All other chemicals and reagents, unless otherwise noted, were obtained from Sigma.

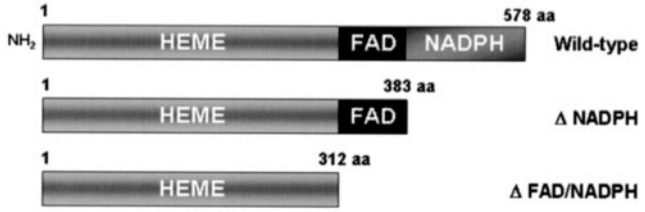

FIG. 1. Schematic structure of Nox4 wild-type and deletion constructs expressed in 3T3-L1 cells by adenoviral gene delivery. The full-length wild-type Nox4 protein is shown with the major functional domains indicated. The construct with the deleted NAD(P)H binding domain is designated ΔNADPH, and the construct with both cofactor domains deleted is indicated as ΔFAD/NADPH.

Cell culture. 3T3-L1 preadipocytes were cultured in Dulbecco's modified Eagle's medium containing 25 mM glucose (DMEM) plus 10% fetal calf serum in a 5% CO_2 atmosphere and were differentiated to adipocytes as previously described (35). Briefly, confluent cells were placed in differentiation medium (DMEM containing 10% fetal bovine serum, 100 nM insulin, 0.25 μM dexamethasone, and 500 μM isobutylmethylxanthine) for 2 days. The medium was then changed to DMEM containing 10% fetal bovine serum and 100 nM insulin. After an additional 6 days of incubation, the cells were used in the indicated experiments.

RT-PCR and Northern blot analysis for NAD(P)H catalytic subunit homologs. Reverse transcription-PCR (RT-PCR) was performed as described by Cheng et al. (8). For Northern analysis, total RNA was isolated from differentiated 3T3-L1 adipocytes using the TRIzol reagent (Invitrogen). Human HepG2 hepatoma cells, human HL-60 promyelocytic leukemia cells, and murine MMC (SV40-transformed glomerular mesangial cells) were used as positive controls for Nox1, Nox2, and Nox4, respectively. RNA was separated electrophoretically on formaldehyde-agarose gels, transferred to Hybond-N$^+$ membrane (Amersham Biosciences), and hybridized with C-terminal cDNA probes of murine Nox1, Nox2, and Nox4 according to the manufacturer's recommendations (NorthernMax; Ambion, Austin, Tex.). cDNA probes were synthesized using the RT-PCR method (Invitrogen) and sequenced before probing to Hybond-N$^+$ membranes to confirm their sequence specificity. Primers used for cDNA probe synthesis were Nox1 (forward, 5′-AAG TGG CTG TAC TGG TTG GG-3′; reverse, 5′-CCA CAT AAG AAA ACC CCC ACC G-3′; cDNA length, 411 bp), Nox2 (forward, 5′-CCA GTG AAG ATG TGT TCA GCT A-3′; reverse, 5′-AGG GTG TTC ACT TGC AAT GGT C-3′; cDNA length, 406 bp), and Nox4 (forward, 5′-GAA GCC CAT TTG AGG AGT CA-3′; reverse, 5′-GGG TCC ACA GCA GAA AAC TC-3′; cDNA length, 409 bp).

Generation of recombinant wild-type and Nox4 deletion constructs in adenoviral vectors. The human wild-type Nox4 cDNA was cloned as described previously (8). cDNA constructs for dominant-negative Nox4 lacking NAD(P)H or FAD-NAD(P)H binding domains were generated by removing C-terminal sequences from the wild-type Nox4 cDNA encoding 578 amino acids (GenBank accession number AF254621) for ΔNAD(P)H (including start codon through 1,150 bp; amino acids 1 to 383) or for ΔFAD-NAD(P)H (start codon through 938 bp; amino acids 1 to 312) (Fig. 1). These cDNA constructs were introduced into defective Ad-5 adenoviruses using the Adeno-X expression system, which is driven by the human cytomegalovirus immediate-early promoter-enhancer and also contains a bovine growth hormone polyadenylation signal, according to the instructions provided by the manufacturer (BD Biosciences). The presence of the intact cDNA inserts was characterized in recombinant adenovirus DNA purified from transfected 293 cells by PCR. Recombinant virus was recovered from a large-scale preparation of adenovirus from 293 cells, and titers were determined using the Adeno-X rapid titer kit (BD Biosciences). A recombinant adenovirus encoding bacterial β-galactosidase was used as control.

Adenoviral transduction of 3T3-L1 adipocytes. 3T3-L1 adipocytes were transduced with recombinant adenovirus according to an established protocol (40). Briefly, after differentiation in 3T3-L1 cells, the various recombinant adenovirus constructs (600 infection-forming units/cell) were preincubated for 100 min at room temperature in DMEM containing 0.5% bovine serum albumin (BSA) and 0.5 μg of polylysine/ml. After preincubation, adenovirus infection of 3T3-L1 adipocytes was performed by overnight incubation in DMEM containing 0.5% BSA. The next day, the medium was replaced with complete medium containing 10% fetal bovine serum and 100 nM insulin; 72 h posttransduction, the cells were used for experiments after starving overnight with serum-free medium.

Detection of the transduced Nox4 deletion constructs was performed by RT-PCR, since the available antibody to Nox4 was directed at a C-terminal protein epitope that is lacking in both of the recombinant constructs. Using reagents provided by Ambion, oligo(dT)-directed RT of cellular RNA was followed by 35 cycles of PCR with a reverse primer (5′-AATGATGGTGACTGGC-3′) and a forward primer (5′-TCTCAGTGAATTACAGT-3′) to generate a Nox4 fragment of 550 bp.

Transfection of siRNAs into 3T3-L1 adipocytes. The following siRNAs were designed to target the murine Nox4 cDNA sequences: siRNA 1 (5′-AACGAA GGGGTTAAACACCTC-3′); siRNA 3 (5′-AAAAGCAAGACTCTACACAT C-3′); scrambled, control siRNA (5′-CAGTCGCGTTTGCGACTGG-3′) (Dharmacon, Inc.). Either 20 nmol of scrambled or siRNA 1 or 3, or 10 nmol each of siRNA 1 and siRNA 3 was electroporated into differentiated 3T3-L1 adipocytes as described elsewhere (6). Briefly, cells were electroporated with siRNA and reseeded in six-well plates; 48 h later, cells were starved for 4 h and stimulated without or with insulin (100 nM) for 5 min prior to lysis with ice-cold buffer containing 50 mM HEPES (pH 7.5), 150 mM NaCl, 1% Triton X-100, 100 mM sodium fluoride, 1 mM EGTA, 1 mM EDTA, 2 mM sodium vanadate, 10 mM sodium pyrophosphate, 1 mM phenylmethylsulfonyl fluoride, and a protease inhibitor cocktail (Sigma). For immunoprecipitation of Nox4 protein, lysates were briefly sonicated and cleared by centrifugation at 13,000 × *g* for 10 min, followed by immunoprecipitation using the polyclonal Nox4 antibody, sodium dodecyl sulfate-polyacrylamide gel electrophoresis (SDS-PAGE), transfer onto polyvinylidene difluoride (PVDF) membranes, and Western blotting with Nox4-specific antibody using standard methods.

The Nox4 antibody was generated from a His-tagged recombinant fragment of human Nox4 encoding the C-terminal amino acids 320 to 428, which has 95% homology with murine Nox4 in that region. After purification on a nickel-nitrilotriacetic acid column (Qiagen), a polyclonal antibody was generated in rabbits. The rabbit antiserum was purified on a protein A column and also passed through a bacterial lysate column (Pierce) to remove nonspecific reactivity with *Escherichia coli* antigens.

Assay of intracellular H_2O_2 in 3T3-L1 adipocytes. Intracellular generation of H_2O_2 was visualized as described previously (2, 5, 35). After wild-type and dominant-negative Nox4 encoding recombinant adenovirus transduction into 3T3-L1 adipocytes, cells were stimulated with insulin (100 nM) for 5 min. Following stimulation, 3T3-L1 adipocytes were washed with minimal essential medium (lacking phenol red) and then incubated in the dark for 10 min with CM-DCF-DA. The fluorescence of CM-DCF-DA was measured by using a Bio-Rad confocal microscope at an excitation wavelength of 488 nm and emission at 515 to 540 nm. To avoid photooxidation of the indicator dye, the fluorescence image was collected by a single rapid scan with identical parameters for all samples. Where indicated, the fluorescence intensity was quantitated from sampled images using Scion Image software (Scion Corporation, Frederick, Md.).

Immunoblotting. After wild-type and dominant-negative Nox4-encoding or wild-type and dominant-negative PTP1B-encoding recombinant adenovirus transduction or siRNA transfection into 3T3-L1 adipocytes, cells were stimulated with insulin for 5 min and then lysed in buffer containing 50 mM HEPES (pH 7.5), 150 mM NaCl, 1% Triton X-100, 100 mM sodium fluoride, 1 mM EGTA, 1 mM EDTA, 2 mM sodium vanadate, 10 mM sodium pyrophosphate, 1 mM phenylmethylsulfonyl fluoride, and a protease inhibitor cocktail (Sigma). The lysates were briefly sonicated and centrifuged at 13,000 × *g* for 10 min, and 75 μg of protein of the cleared supernatant was resolved by SDS-PAGE and transferred to PVDF membrane using a semidry Western blotting apparatus (AP Biotech). PVDF membranes were subjected to immunoblotting with either monoclonal antibody for phosphotyrosine (4G10) to detect insulin receptor β-subunit and IRS tyrosine phosphorylation, polyclonal antibody to detect phospho-Akt, and monoclonal antibody to detect phospho-Erk1/2 MAPK, or additional antibodies to detect total protein levels of the insulin receptor β-subunit, IRS-1, Akt, and ERK1/2 MAPK where indicated. Following incubation with horseradish peroxidase-conjugated secondary antibodies, proteins were visualized by ECL according to the instructions provided by the manufacturer. The immunoblotting signals were quantitated using an ImageStation 440 (Kodak). Protein was measured by the method of Bradford (7).

Immunoprecipitation of IRS-1 to assess p85 (PI 3′-kinase subunit) binding. Cell treatments and preparation of lysates from 3T3-L1 adipocytes were performed as described above. Briefly, cells were serum starved overnight in DMEM containing 0.5% BSA. After stimulation with insulin as indicated, cells were snap-frozen with liquid nitrogen and lysed in ice-cold lysis buffer. The lysates were briefly sonicated and centrifuged at 15,000 × *g* for 10 min. After normalizing the protein concentration, cleared lysates were incubated with IRS-1 antibody overnight at 4°C. The samples were then incubated for 2 h with a 50% (vol/vol) slurry of protein A-agarose at 4°C, pelleted by centrifugation in a microcentrifuge, and washed three times with ice-cold lysis buffer. SDS gel sample buffer was then added, and the samples were heated to boiling, processed by SDS gel electrophoresis, and transferred to PVDF membranes. Membranes were probed overnight with antibody to the p85 noncatalytic subunit of PI 3′-kinase. Following incubation with horseradish peroxidase-conjugated secondary antibodies, bound antibody was detected using ECL. To reprobe the blot, the membrane was incubated for 30 min at 50°C in stripping buffer (62.5 mM Tris-HCl [pH 6.8], 100 mM 2-mercaptoethanol, and 2% SDS) and then washed several times with TBST (20 mM Tris-HCl [pH 7.6], 137 mM NaCl, and 0.1% Tween 20). The PVDF membrane was reprobed with the IRS-1 antibody, and bound antibody was detected as described above.

Glucose uptake in 3T3-L1 adipocytes. Adenovirus-transduced or siRNA-transfected 3T3-L1 adipocytes were starved for serum for 4 h, washed with KRPH buffer (5 mM Na_2HPO_4, 20 mM HEPES [pH 7.4], 1 mM $MgSO_4$, 1 mM $CaCl_2$, 136 mM NaCl, 4.7 mM KCl, 0.2% [wt/vol] BSA), and treated with 100 nM insulin in KRPH buffer where indicated. Following 11 min of incubation with insulin, glucose uptake was assessed by the addition of 100 μM 2-deoxy-D-glucose containing 0.5 μCi of [^{3}H]2-deoxy-D-glucose as described previously (14). The reaction was stopped 4 min later by washing the cells three times with ice-cold phosphate-buffered saline. The cells were then solubilized in 0.05% (wt/vol) SDS at 37°C for 30 min, and aliquots were subjected to scintillation counting. Nonspecific uptake (<10% of the total) was determined in the presence of cytochalasin B (50 μM) and was subtracted from the total uptake.

Specific activity of PTP1B. Under strictly anaerobic conditions to preserve the endogenous level of catalytic activity and avoid air oxidation (47), PTP1B was immunoprecipitated from lysates of transduced 3T3-L1 adipocytes (375 μg of protein) with a monoclonal antibody directed at a C-terminal epitope that preserves its enzymatic activity (Ab-2) followed by adsorption to Tris-acryl protein G. PTPase activity was measured by the hydrolysis of *para*-nitrophenyl phosphate in the anaerobic chamber in washed immunoprecipitates as our investigators have reported previously (35). The reaction was terminated by the addition of 50 μl of 1 M NaOH, and the absorption was determined at 410 nm.

Statistical analyses. Quantitative data are presented as the mean ± standard error of the mean for three to five experiments. Statistical analysis was based on Student's *t* test for comparison of two groups and one-way analysis of variance for multiple group comparisons. A *P* value less than 0.05 was used to determine statistical significance.

RESULTS

Expression of Nox family homologs in insulin-sensitive cells. Using RT-PCR techniques as reported previously (8), we identified relatively high expression of Nox4 in human subcutaneous and omental adipose tissue, human HepG2 hepatoma cells, and SV40-transformed human endothelial (HAD-MEC-5) cells compared to other Nox family homologs, including Nox1, Nox2, Nox3, Nox5, Duox1, and Duox2 (Fig. 2A). We then confirmed the relatively high abundance of Nox4 mRNA and undetectable mRNA expression for Nox1 and Nox2 in differentiated 3T3-L1 adipocytes by RT-PCR and Northern blot analysis, using positive control cell lines known to express the candidate Nox homologs (Fig. 2B and C). The expression of Nox2 in the adipose tissue samples shown in Fig. 2A is likely due to the presence of this abundant leukocyte homolog (gp91*phox*) in trapped blood cells that were captured in the RNA sample.

Protein expression of Nox4 in 3T3-L1 cells was confirmed using a specific antibody for Nox4 made to a recombinant protein antigen encoding the C-terminal region of the protein (Fig. 3A). These data raised the possibility that the NAD(P)H oxidase homolog Nox4 might play a role in insulin-stimulated oxidant production in adipose cells.

Expression of recombinant Nox4 constructs and PTP1B in 3T3-L1 adipocytes. In order to test this hypothesis more directly, we used adenovirus-mediated gene delivery to overexpress recombinant Nox4 constructs including wild-type and

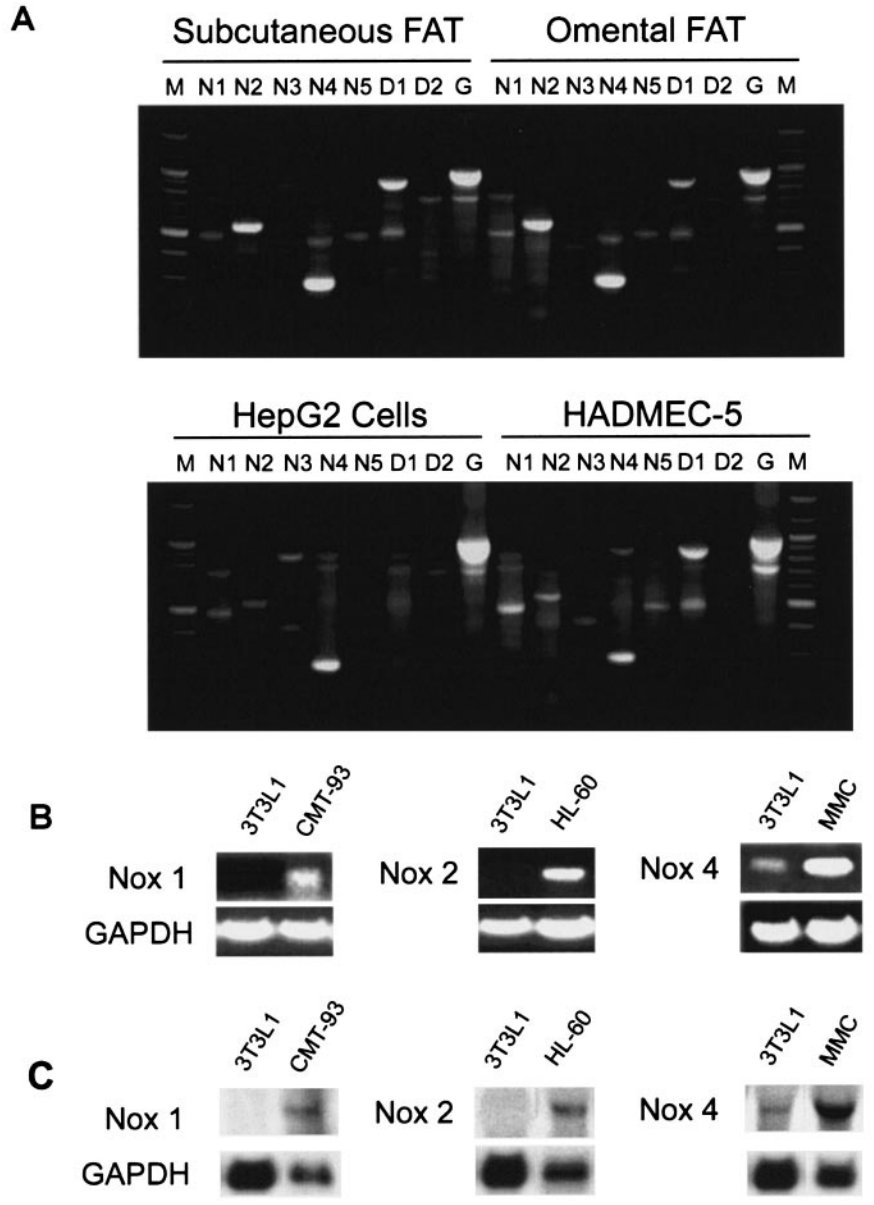

FIG. 2. Expression of Nox family homologs in adipose tissue and various cultured cells. (A) RT-PCR of Nox family homologs. Total RNA was prepared using the TRIzol reagent, and RT-PCR was performed with primers specific for human Nox1, Nox2, Nox3, Nox4, Nox5, Duox1, and Duox2 in human subcutaneous and omental adipose tissue, HepG2 hepatoma cells, and SV40-transformed human microvascular endothelial (HADMEC-5) cells using previously reported techniques (8). N1 to N5, Nox1 to Nox5; D1 and D2, Duox 1 and 2; G, glyceraldehyde-3-phosphate dehydrogenase (GAPDH) as an internal control; M, molecular size markers. (B) RT-PCR was performed using RNA isolated from differentiated 3T3-L1 adipocytes as described in Materials and Methods using primers for PCR analysis that were specific to murine Nox family homologs Nox1, Nox2, and Nox4. Control cell lines included CMT-93 (murine colon carcinoma cells), HL-60 (human leukemia cells), and MMC (murine mesangial cells). (C) Northern blot analysis of Nox4 mRNA expression in differentiated 3T3-L1 adipocytes. Total RNA was isolated from the indicated cells using the TRIzol reagent, and Northern blot analysis using Nox1-, Nox2-, and Nox4-specific cDNA probes or GAPDH as a loading and transfer control was performed as described in Materials and Methods.

two deletion mutants, one lacking the NAD(P)H binding domain and the other lacking both the FAD and NAD(P)H binding domains, as well as a recombinant β-galactosidase construct as control. Seventy-two hours postinfection, no cytotoxicity was apparent in the cells transduced with any of the constructs. Since the only available Nox4 antibody was directed at the C-terminal heme binding domain of Nox4, we could not perform Western blotting to characterize the level of expression of the recombinant constructs. However, expression of mRNA for each of the transduced Nox4 constructs was detected using RT-PCR (Fig. 3B). The predicted 550-bp cDNA band revealed comparable expression of wild-type human Nox4 as well as the two deletion constructs expressed in 3T3-L1 adipocytes. Since the PCR primers were homologous

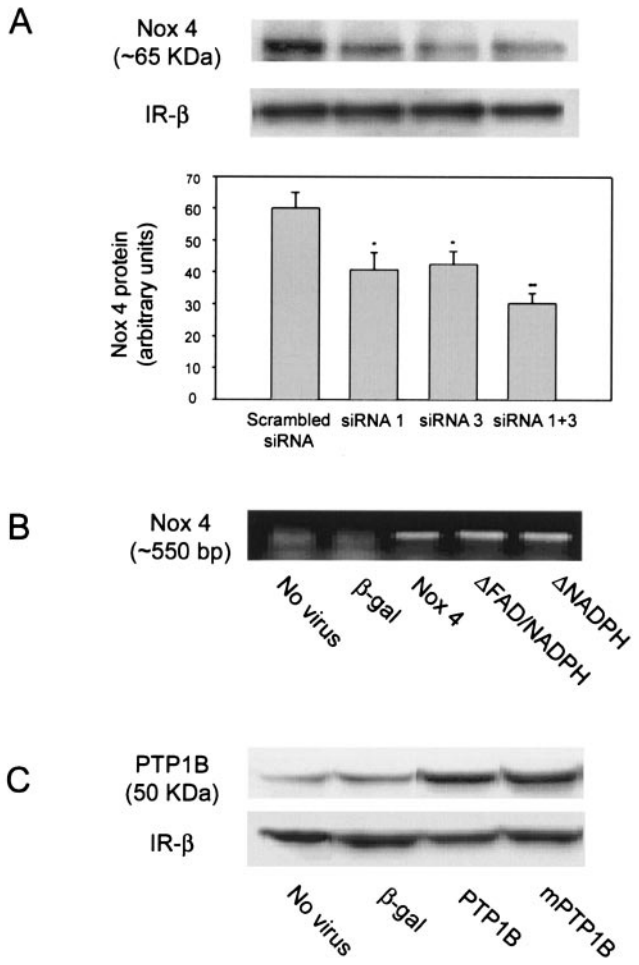

FIG. 3. Expression of Nox4 protein in 3T3-L1 adipocytes after transfection of siRNA oligonucleotides and expression of recombinant Nox4 mRNA and PTP1B protein in 3T3-L1 adipocytes following adenovirus-mediated gene delivery. (A) 3T3-L1 adipocytes were transfected with Nox4-specific (siRNA 1, 3, or both together) or a scrambled control siRNA oligonucleotide and reseeded in six-well plates (6). After 48 h of incubation, cell lysates were prepared and incubated with Nox4 polyclonal antibody to immunoprecipitate Nox4 protein. Immunoprecipitates were separated by SDS-PAGE and reblotted with Nox4 antibody as described in Materials and Methods. A representative blot demonstrating expression of Nox4 protein at ~65 kDa and a reduction in Nox4 abundance following loading of specific siRNA oligonucleotides is shown. Protein expression for the insulin receptor β-subunit is shown as an experimental control. The bar graph shows mean data from replicate immunoblots quantitated using ImageStation 440 (Kodak). *, $P = 0.05$; **, $P = 0.01$ versus control cells transfected with the scrambled siRNA. (B) At 72 h following transduction of differentiated 3T3-L1 adipocytes with adenovirus encoding β-galactosidase or the indicated Nox4 constructs, total RNA was prepared using the TRIzol reagent and RT-PCR was performed with Nox4-specific primers as described in Materials and Methods. Nox4 was detected as a ~550-bp band in the ethidium bromide-stained agarose gel. (C) Cell lysates were prepared from 3T3-L1 cells 72 h after transduction with control adenovirus encoding β-galactosidase, wild-type PTP1B, or a site-directed catalytically inactive (Cys^{215}→Ser) PTP1B construct (mPTP1B). Proteins were separated by SDS-PAGE and immunoblotted with PTP1B antibody as described in Materials and Methods. The 50-kDa PTP1B protein band is indicated. Protein expression for the insulin receptor β-subunit is shown as an experimental control.

only to the transduced human Nox4 sequence, no cDNA band was detected in the nontransduced or the β-galactosidase-transduced murine 3T3-L1 adipocytes.

For comparison with the studies on the effects of Nox4, 3T3-L1 adipocytes were also transduced with recombinant wild-type human PTP1B and a site-directed catalytically inactive mutant enzyme (Cys^{215}→Ser) using the same adenovirus system (12). By Western blot analysis, the level of PTP1B protein in the transduced 3T3-L1 adipocytes was increased 10- to 15-fold compared with cells transduced with the β-galactosidase-encoding adenovirus (Fig. 3C).

Effect of expression of recombinant Nox4 and PTP1B on the insulin-induced oxidant signal. Insulin-stimulated generation of cellular reactive oxygen species was measured in the transduced 3T3-L1 adipocytes after loading with the sensitive fluorescent oxidant indicator dye CM-DCF-DA (35). At 72 h postadenoviral infection, adipocytes were stimulated with 100 nM insulin for 5 min, and in control cells a rapid increase in intracellular DCF fluorescence was detected within 1 min using confocal microscopy (Fig. 4). Compared to controls (either uninfected or those infected with recombinant β-galactosidase), insulin-induced DCF fluorescence was increased by 21% ($P = 0.02$) in cells overexpressing wild-type Nox4. Importantly, insulin-induced oxidant generation was sharply attenuated by 72 to 75% in cells transduced with either of the Nox4 deletion constructs ($P < 0.001$). These findings are consistent with the deletion constructs acting in a dominant-negative fashion to inhibit insulin-induced oxidant generation, and they provide strong evidence that the NAD(P)H oxidase system in adipocytes involves the catalytic activity of Nox4. In parallel, overexpression of wild-type PTP1B, but not the catalytically inactive mutant, suppressed insulin-stimulated oxidant generation to a similar extent as the Nox4 deletion constructs, further suggesting that the post-insulin receptor signal transduction cascade is largely coupled to the generation of the oxidant signal (Fig. 4).

Effects of expression of recombinant Nox4 and PTP1B constructs on insulin receptor and IRS tyrosine phosphorylation. The effects of Nox4 or PTP1B on insulin-induced tyrosine phosphorylation of the insulin receptor (Fig. 5A) and IRS-1/2 (Fig. 5B) were then assessed using Western blot analysis with antiphosphotyrosine antibody. In untransduced cells, insulin stimulation for 5 min increased insulin receptor tyrosyl phosphorylation by five- to sixfold and IRS-1/2 tyrosyl phosphorylation by three- to fourfold. Adenovirus-directed β-galactosidase expression had no effect on basal or insulin-stimulated insulin receptor or IRS-1/2 tyrosyl phosphorylation. Overexpression of wild-type Nox4 or inactive PTP1B did not affect basal or insulin-stimulated insulin receptor or IRS protein tyrosine phosphorylation. In cells expressing either of the dominant-negative Nox4 constructs, however, insulin-stimulated phosphorylation was decreased by 46 to 56% for the insulin receptor ($P = 0.001$) and 28 to 58% for the IRS proteins ($P = 0.01$) versus control cells transduced with β-galactosidase. For comparison, wild-type PTP1B transduction sharply reduced the insulin-stimulated tyrosine phosphorylation of the insulin receptor-β subunit and IRS-1/2 proteins by 65% ($P < 0.001$) and 73% ($P < 0.001$), respectively.

Effect of siRNA-induced reduction of Nox4 protein mass on insulin-stimulated insulin receptor tyrosine phosphorylation.

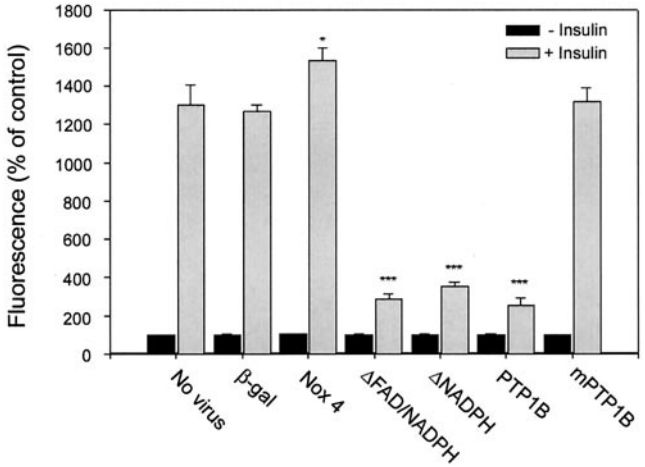

FIG. 4. Effect of adenoviral expression of recombinant Nox4 and PTP1B constructs on insulin-stimulated production of H_2O_2 in 3T3-L1 adipocytes. Seventy-two hours after transduction with the indicated adenovirus constructs, differentiated 3T3-L1 adipocytes were starved overnight in serum-free medium, loaded with CM-DCF-DA, and stimulated with 100 nM insulin for 5 min as described in Materials and Methods. Intracellular H_2O_2 production was detected by fluorescence of DCF in situ using confocal microscopy as reported previously (35). *, $P = 0.02$; ***, $P < 0.001$ versus control.

To provide confirmatory evidence into the potential role of Nox4 in the insulin signaling pathway, we also performed experiments in which Nox4 protein abundance was reduced by loading 3T3-L1 adipocytes with siRNA constructs directed at murine Nox4. Forty-eight hours after transfection, immunoprecipitation of Nox4 and Western blotting demonstrated that loading with siRNA 1 or siRNA 3 resulted in a 32 and 30% ($P = 0.05$) decrease in Nox4 protein mass, respectively, while cells transfected with a mixture of both siRNAs had a decrease in Nox4 protein to 50% ($P = 0.01$) of the control level in cells transfected with a scrambled, control siRNA preparation (Fig. 3A). There was no change in the mass of the insulin receptor β-subunit, which was used as an internal control.

Following stimulation with insulin, the siRNA-transfected cells with reduced endogenous Nox4 expression demonstrated a 49 to 64% ($P = 0.01$) decrease in insulin receptor tyrosyl phosphorylation compared to the control cells transfected with the scrambled siRNA controls (Fig. 5D). Thus, cellular reduction of Nox4 protein abundance significantly affected the initiation of the insulin signaling cascade to a similar degree as the dominant-negative effects of the transduced Nox4 deletion constructs (Fig. 5A).

Effect of expression of recombinant Nox4 constructs and wild-type PTP1B on PI 3′-kinase p85 subunit binding to IRS-1. We next assessed whether the effects of Nox4 affected downstream insulin signaling to the PI3′-kinase pathway in the 3T3-L1 cells (Fig. 6). Overexpression of wild-type Nox4 itself did not significantly affect the insulin-stimulated association between the p85 subunit of PI 3′-kinase and IRS-1. However, in cells overexpressing the Nox4 FAD-NAD(P)H deletion construct or wild-type PTP1B, the stimulation of the p85 subunit association with IRS-1 was reduced by 30 to 33% compared to control ($P < 0.001$).

Effect of transfection of Nox4 siRNA on insulin-stimulated Akt phosphorylation. To evaluate whether a reduction in Nox4 mass affected insulin signaling to downstream kinases, 48 h after loading with Nox4 siRNA, cells were starved for 4 h in DMEM with 0.5% BSA and then treated with 100 nM insulin for 5 min. Immunoblotting of cell lysates with phospho-Akt-specific polyclonal antibody revealed that insulin stimulated a six- to sevenfold increase in Akt phosphorylation in control cells transfected with the scrambled siRNA. In cells transfected with the Nox4-specific siRNA, however, insulin-stimulated Akt phosphorylation was decreased by 35 to 48% ($P = 0.007$) compared to the control response (Fig. 7).

Effect of expression of recombinant Nox4 and PTP1B constructs on Erk1 and Erk2 MAPK activation. Compared to cells transduced with the control adenovirus, insulin-stimulated phosphorylation of both Erk1 and Erk2 was decreased by 41 to 59% ($P = 0.02$) in cells expressing the Nox4 deletion constructs and decreased by 38% ($P = 0.002$) in the cells overexpressing wild-type PTP1B (Fig. 8). Overexpression of wild-type Nox4 or the inactive PTP1B had no effect on insulin-stimulated Erk phosphorylation, and the amount of Erk protein was not altered by the cell transductions.

Effect of expression of Nox4 cDNA constructs and siRNA on insulin-stimulated glucose uptake. In cells transduced with the control adenovirus, the basal glucose uptake in 3T3-L1 adipocytes was increased by 30% and was increased ~2-fold with each of the recombinant Nox4 deletion constructs (Fig. 9A). Following insulin stimulation, glucose uptake was increased by 3.9- and 3.0-fold over the basal level in the control, untransduced cells and in the β-galactosidase-transduced controls, respectively. In the wild-type Nox4-overexpressing cells, the level of insulin-stimulated glucose uptake was increased by 22% over the level in control cells ($P = 0.05$), but due to the increase in basal uptake the degree of stimulation was reduced to 2.4-fold. In 3T3-L1 adipocytes overexpressing the dominant-negative Nox4 ΔFAD-NAD(P)H construct, the level of insulin-stimulated glucose transport was decreased by 32% compared to the wild-type overexpressing cells ($P = 0.001$), and the level of insulin stimulation was markedly reduced to only 1.7-fold compared to controls. Changes in insulin-stimulated glucose uptake with the Nox4 ΔNAD(P)H construct were at an intermediate level.

3T3-L1 adipocytes electroporated with the control, scrambled siRNA construct showed relatively high basal glucose transport that was increased by 37% with insulin stimulation (Fig. 9B). Cells transfected with the active Nox4 siRNAs exhibited a 30 to 44% reduction in basal glucose transport and a similar drop in the level of insulin-stimulated glucose uptake. Taken together with the Nox4 transduction studies noted above, these results suggest that Nox4 overexpression helps potentiate, and a reduction in Nox4 mass reduces, the level of insulin-stimulated glucose transport in 3T3-L1 adipocytes.

Role of Nox4 in the modulation of insulin receptor tyrosine phosphorylation by PTP1B. In order to determine if Nox4 interacted with PTP1B in its effect on insulin signal transduction, we cotransduced two recombinant adenoviruses to increase the level of expression of PTP1B and wild-type Nox4 or the dominant-negative ΔFAD-NAD(P)H construct (Fig. 5C). As described above and shown in Fig. 5A, overexpression of PTP1B alone reduced the insulin-stimulated autophosphory-

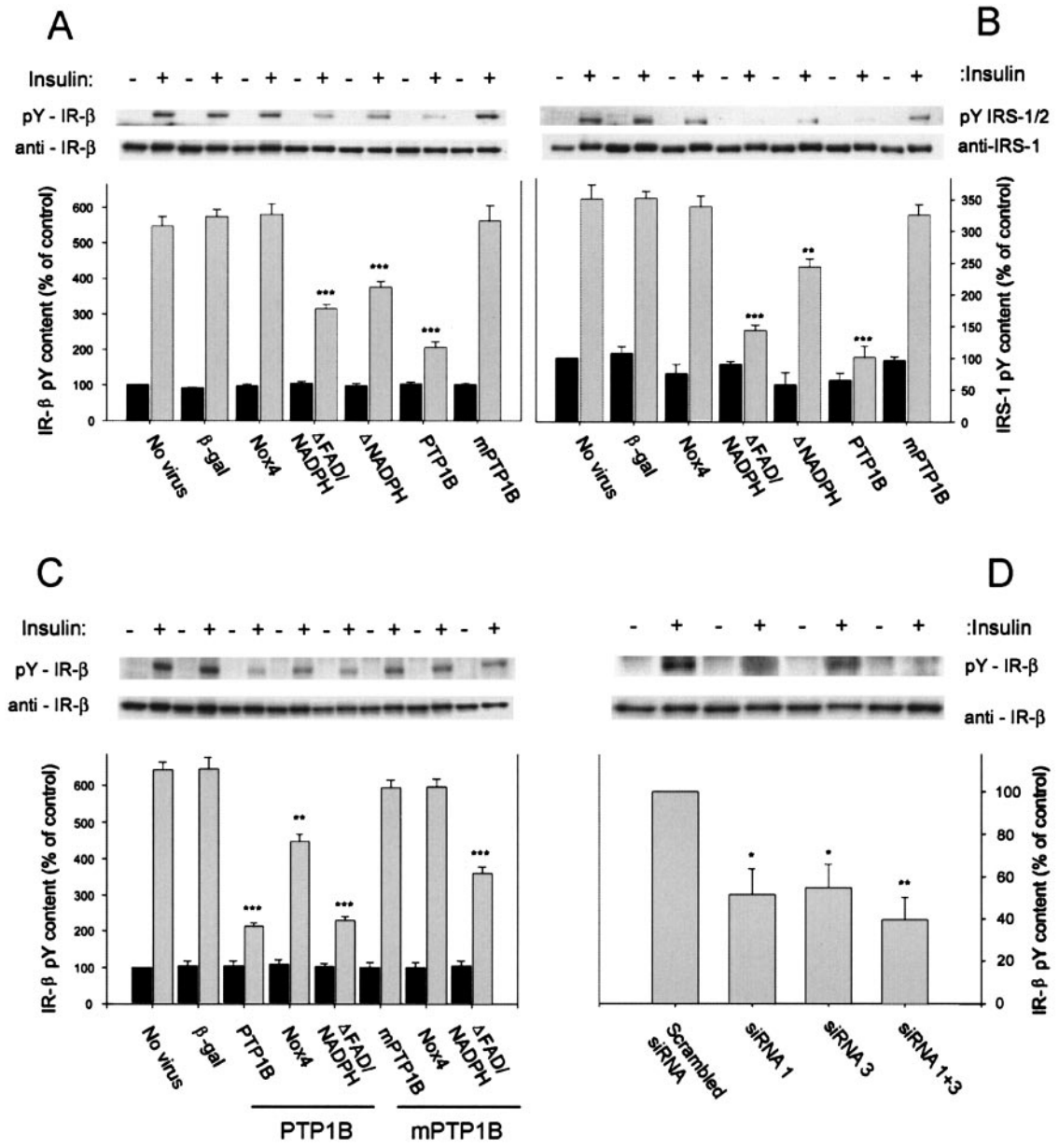

FIG. 5. Effect of adenoviral expression of recombinant Nox4 and PTP1B constructs on insulin-stimulated tyrosine phosphorylation of the insulin receptor β-subunit and IRS proteins. (A) Representative antiphosphotyrosine (4G10) and anti-insulin receptor β-subunit immunoblots of 3T3-L1 cell lysates transduced with adenovirus encoding wild-type Nox4 as well as two dominant-negative constructs lacking binding domains for NAD(P)H or FAD/NAD(P)H or wild-type PTP1B and mutant PTP1B, following stimulation of serum-starved cells with 100 nM insulin for 5 min. The migration positions of the tyrosine-phosphorylated insulin receptor β-subunit (95 kDa) are indicated as pY-IR-β. Mean data for the phosphotyrosine density of the insulin receptor β-subunit from replicate immunoblots quantitated using an ImageStation 440 (Kodak) are shown in the bar graph. ***, $P \leq 0.001$ versus control β-galactosidase-encoding adenovirus-transduced 3T3-L1 adipocytes. (B) Samples identical to those described in the legend for panel A were analyzed for phosphotyrosine content of IRS1/2 and IRS1 protein using antiphosphotyrosine antibodies (4G10) and IRS-1 antibody following stimulation of serum-starved cells with 100 nM insulin for 5 min. The migration positions of the tyrosine-phosphorylated IRS1/2 (~ 185 kDa) are indicated as pY IRS-1/2. Mean data for the phosphotyrosine density of IRS-1/2 from replicate immunoblots are shown in the bar graph. **, $P = 0.01$; ***, $P \leq 0.001$ versus control cells transduced with the β-galactosidase-encoding adenovirus. (C) Representative antiphosphotyrosine (4G10) and anti-insulin receptor β-subunit immunoblots of 3T3-L1 cell lysates transduced with adenovirus encoding wild-type PTP1B or mutant PTP1B and cotransduced with adenovirus encoding Nox4 or the FAD/NAD(P)H Nox4 deletion construct where indicated, following stimulation of serum-starved cells with 100 nM insulin for 5 min. Mean data for the phosphotyrosine density of the insulin receptor β-subunit from replicate immunoblots are shown in the bar graph. **, $P = 0.01$; ***, $P \leq 0.001$ versus control cells transduced with the β-galactosidase-encoding adenovirus. (D) Effect of reduction of Nox4 mass on insulin-stimulated tyrosine phosphorylation of the insulin receptor β-subunit, as shown in representative antiphosphotyrosine (4G10) and anti-insulin receptor β-subunit (IR-β) immunoblots of 3T3-L1 cell lysates transfected with control (scrambled) or Nox4-specific siRNA oligonucleotides. Following stimulation of serum-starved cells with 100 nM insulin for 5 min, cell lysates were prepared and SDS-PAGE and immunoblotting were performed. Mean data for the phosphotyrosine density of the insulin receptor β-subunit from replicate immunoblots are shown in the bar graph. *, $P = 0.05$; **, $P = 0.01$ versus control transfected 3T3-L1 adipocytes.

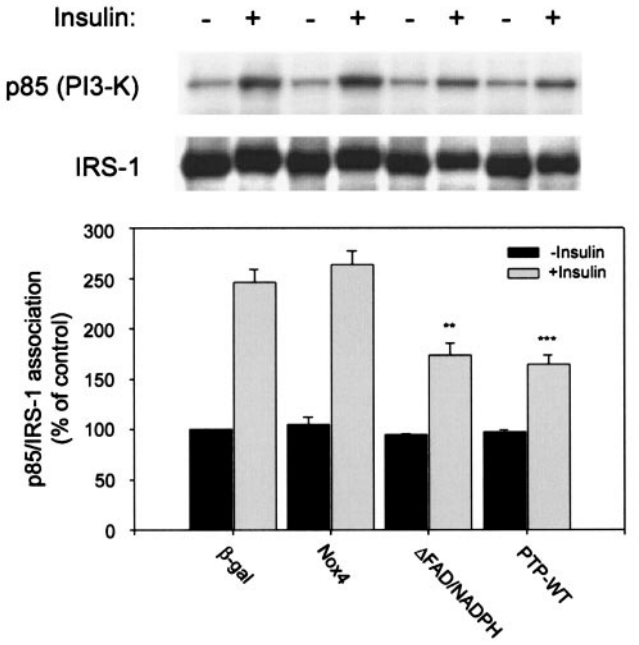

FIG. 6. Effect of adenoviral expression of Nox4 deletion constructs and wild-type PTP1B on the association of the p85 subunit of PI 3′-kinase with IRS-1. Transduction of 3T3-L1 adipocytes with adenovirus, stimulation of cells with insulin, and preparation of lysates were performed as described in the legend to Fig. 4. After immunoprecipitation of IRS-1 from the lysates as described in Materials and Methods, samples were separated by gel electrophoresis, transferred to PVDF membranes, and probed overnight with antibody to the p85 noncatalytic subunit of PI 3′-kinase. After stripping, PVDF membranes were reprobed with the IRS-1 antibody for normalization. The upper panel shows a representative immunoblot, and the bar graph in the lower panel represents the p85 subunit binding to IRS-1 protein from replicate immunoblots after quantitation. **, $P < 0.01$; ***, $P < 0.001$ versus control β-galactosidase-encoding adenovirus-transduced 3T3-L1 adipocytes.

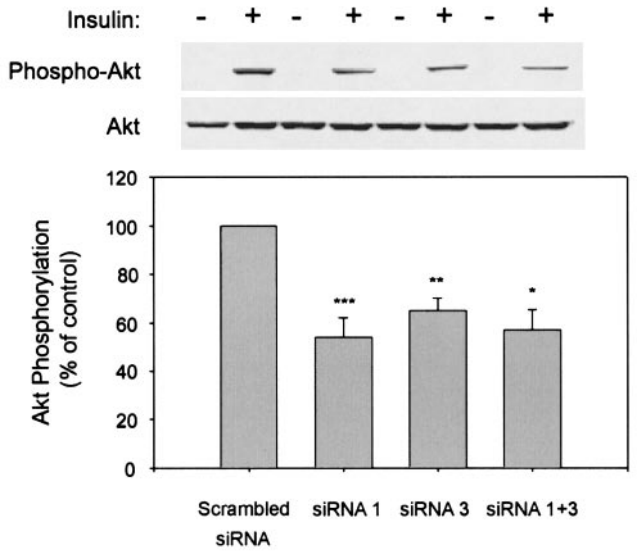

FIG. 7. Effect of siRNA-induced reduction of Nox4 protein mass on insulin-stimulated Akt phosphorylation in 3T3-L1 adipocytes. Results shown are representative anti-phospho-Akt and anti-Akt protein immunoblots of 3T3-L1 cell lysates from cells transfected with control (scrambled) or Nox4-specific siRNA oligonucleotides and following stimulation of serum-starved cells with 100 nM insulin for 5 min as described in Materials and Methods. The bar graph represents mean data from replicate immunoblots after quantitation of signal density. *, $P = 0.05$; **, $P = 0.01$; ***, $P = 0.007$ versus control 3T3-L1 adipocytes transfected with the scrambled siRNA.

lation of the insulin receptor by 67%. Cooverexpression of Nox4 along with PTP1B significantly diminished the effect of PTP1B alone on insulin receptor β-subunit tyrosine phosphorylation by 46%. When cooverexpressed, the ΔFAD-NAD(P)H construct had no significant effect on the reduction of insulin-stimulated receptor tyrosine phosphorylation by PTP1B overexpression (Fig. 5C).

In control experiments, neither overexpression of catalytically inactive PTP1B (mPTP1B) alone nor cotransduction of Nox4 along with mPTP1B affected insulin receptor autophosphorylation (Fig. 5C), as observed in our studies described above (Fig. 5A). In addition, cotransduction the ΔFAD-NAD(P)H deletion construct along with mPTP1B inhibited insulin receptor tyrosine phosphorylation by 40%, suggesting that the underlying interaction between the dominant-negative Nox4 homolog and the endogenous active PTP1B was retained, similar to the experiments shown in Fig. 5A.

Role of Nox4 in the modulation of PTP1B catalytic activity. To determine whether Nox4 overexpression affected the activity of PTP1B, we transduced 3T3-L1 cells with active PTP1B with and without cotransduction with active Nox4 and measured PTP1B activity specifically in immunoprecipitates using anaerobic conditions to avoid artifactual enzyme oxidation and inhibition by air exposure (Fig. 10). As our investigators reported previously (35), insulin stimulation inhibited the endogenous activity of PTP1B in 3T3-L1 cells by ~50%, and viral infection with the recombinant virus encoding β-galactosidase had no nonspecific effects in control studies. In the absence of insulin stimulation, transduction of recombinant human PTP1B increased the activity in the immunoprecipitates by 52%, which was reduced by 53% in the cells that were cotransduced with the Nox4 enzyme. In the cells overexpressing PTP1B without or with cotransduction of Nox4, insulin stimulation reduced PTPase activity in the PTP1B immunoprecipitates by 16 and 23%, respectively. These findings reveal a clear association between the activity of PTP1B as isolated from the intact cells and the activity of Nox4.

DISCUSSION

Many years prior to the identification of the insulin receptor and the elucidation of its molecular mechanism of signal transduction involving receptor and substrate protein tyrosine phosphorylation, researchers had recognized that small oxidant molecules and reagents that generated H_2O_2 in the cell culture medium could mimic insulin action on glucose transport in adipose cells (10, 33). The early studies of oxidants in insulin signaling also demonstrated that H_2O_2 was actually elaborated during treatment of cells with physiological levels of insulin, raising the possibility that cellular H_2O_2 generation was coupled to insulin stimulation (11, 36). Studies from different laboratories have since shown similar effects of other hormones, growth factors, and cytokines on the generation of

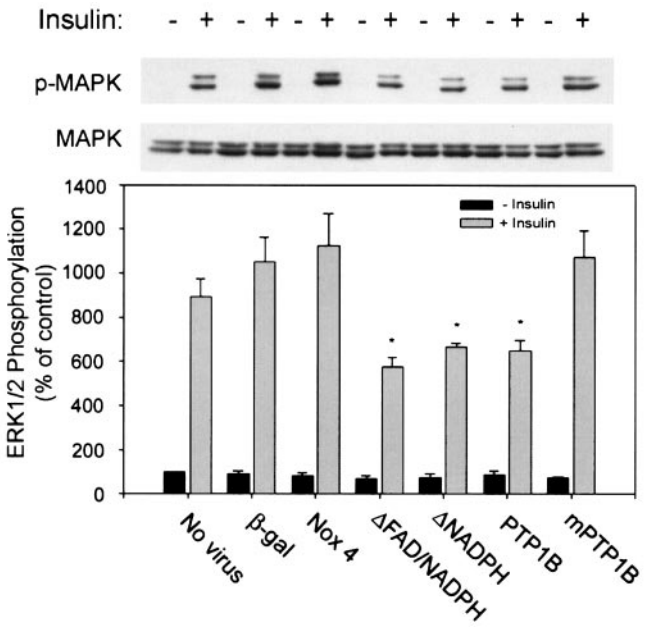

FIG. 8. Effect of adenoviral expression of recombinant Nox4 and PTP1B constructs on Erk1 and Erk2 MAPK activation in 3T3-L1 adipocytes. Representative anti-phospho-MAPK and anti-MAPK protein immunoblots of lysates from 3T3-L1 cells transduced with the indicated adenoviral constructs are shown. Following stimulation of serum-starved cells with 100 nM insulin for 5 min, cell lysates were prepared and immunoblotting was performed with a monoclonal antibody to detect phospho-MAPK (ERK1/2) or anti-MAPK protein antibody. (Upper panel) Representative immunoblots demonstrating the phosphorylation state of MAPK and the MAPK protein level. (Lower panel) Mean data from replicate immunoblots as shown in the upper panel after quantitation of signal density. *, $P = 0.05$ versus control β-galactosidase-encoding adenovirus-transduced 3T3-L1 adipocytes.

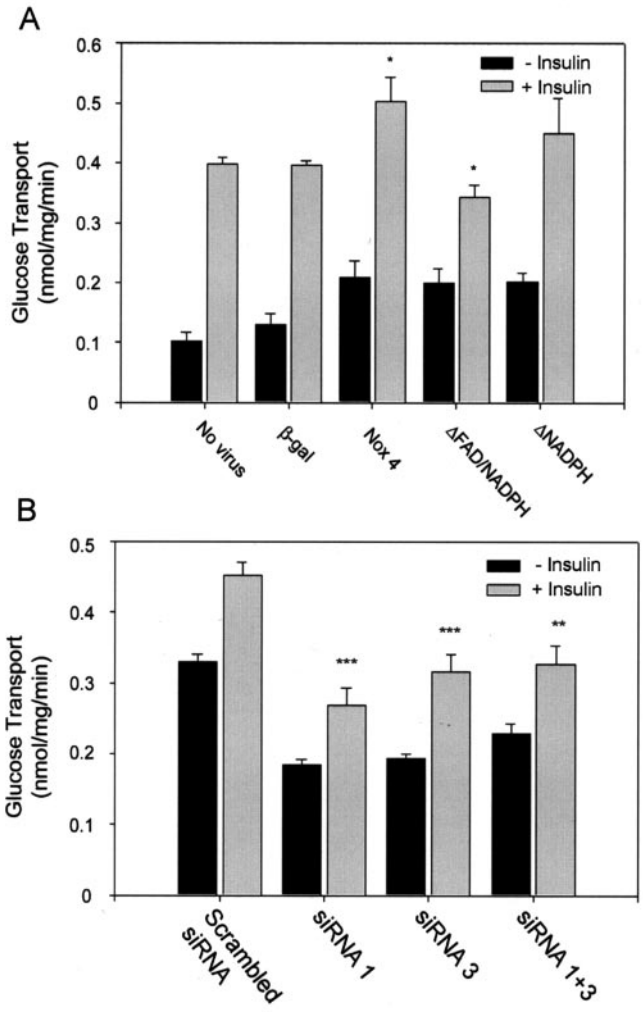

FIG. 9. Effect of adenoviral expression of recombinant Nox4 or PTP1B or siRNA-induced reduction in Nox4 protein mass on insulin-stimulated glucose uptake in 3T3-L1 adipocytes. (A) After differentiation, 3T3-L1 adipocytes were transduced with adenovirus encoding β-galactosidase as a control, wild-type Nox4, or constructs lacking binding domains for NAD(P)H or FAD/NAD(P)H as shown and serum starved for 2 h prior to stimulation with 100 nM insulin and measurement of glucose transport by the uptake of 2-deoxy-D-glucose as described in Materials and Methods. (B) Glucose transport measured in differentiated 3T3-L1 cells after transfection with control (scrambled) or Nox4-specific siRNA oligonucleotides as shown. *, $P < 0.05$; **, $P < 0.01$; ***, $P < 0.001$ versus control cells stimulated with insulin.

reactive oxygen species and their potential involvement in signaling pathways in a variety of effector cell types (3, 15, 20, 21). In their initial biochemical characterization of this process, Mukherjee and Lynn provided evidence that adipocyte plasma membranes contained an NAD(P)H oxidase activity that was activated by insulin (38). Later, Krieger-Brauer and colleagues further demonstrated that within minutes, physiological concentrations of insulin stimulated H_2O_2 production by isolated human fat cells due to a plasma membrane-bound Mn^{2+}-dependent NAD(P)H oxidase enzyme (26, 28) that was also present in 3T3-L1 adipocytes (27).

In the present work, we have initiated a molecular approach to the identification of the insulin-stimulated cellular NAD(P)H oxidase activity expressed in the insulin-sensitive 3T3-L1 adipocyte model system. The identification of a small subfamily consisting of five mammalian NAD(P)H oxidase catalytic subunits (Nox1 to Nox5) homologous to the catalytic subunit of the respiratory burst oxidase, an NAD(P)H-dependent, superoxide-generating enzyme present in phagocytes known as gp91*phox* or Nox2 has facilitated our testing of the potential involvement of individual candidate enzymes as effectors of the insulin-stimulated cellular production of H_2O_2 (8). Each of the Nox family gp91*phox* homologs encodes a protein of ~65 kDa and contains five to six conserved predicted transmembrane α-helices containing putative heme binding regions and a flavoprotein homology domain containing predicted binding sites for both FAD and NAD(P)H. The Nox homologs exhibit unique patterns of cellular expression: Nox1 is predominantly expressed in colon and vascular smooth muscle cells; Nox3 is expressed primarily in fetal tissues; Nox4 is expressed in kidney, placenta, and glioblastoma cells; and Nox5 is expressed in spleen and uterus (8). Since we found that Nox4 mRNA expression was relatively abundant in adipose tissue, 3T3-L1 adipocytes, and HepG2 hepatoma cells (unpublished data), in the present work we evaluated whether Nox4 played a role in cellular insulin-induced oxidant production and insulin signaling. Indeed, using Nox4 deletion constructs

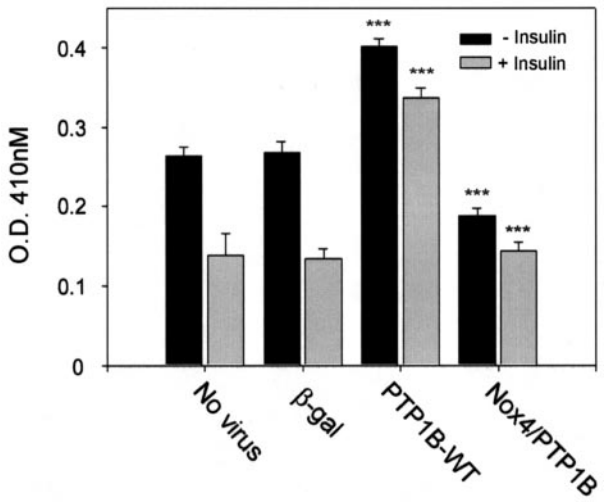

FIG. 10. Effect of adenoviral expression of recombinant PTP1B without or with Nox4 on the endogenous catalytic activity of PTP1B in 3T3-L1 adipocytes. Differentiated 3T3-L1 adipocytes were transduced with adenovirus encoding β-galactosidase as a control or wild-type PTP1B without or with cotransduction of recombinant active Nox4 as shown. Cells were serum starved for 2 h prior to stimulation with 100 nM insulin for 5 min. Cell lysates were immunoprecipitated with a specific antibody for PTP1B, and PTPase activity of the adsorbed enzyme was measured under an insert atmosphere by hydrolysis of *para*-nitrophenyl phosphate as described in Materials and Methods. ***, $P < 0.001$ versus the respective control samples without or with insulin.

that function in a dominant-negative fashion as well as confirmatory studies using siRNA loading to reduce Nox4 abundance, our data indicate clearly that Nox4 is involved in the generation of H_2O_2 by insulin stimulation of differentiated 3T3-L1 adipocytes.

In addition to effects on insulin-stimulated H_2O_2 generation, manipulation of Nox4 impacts significantly on both early and late events in insulin signal transduction, including insulin-stimulated insulin receptor and IRS-1 tyrosine phosphorylation, and the activation of downstream serine kinases and glucose uptake. Thus, the effects of Nox4 on insulin signaling are likely to be mediated by its effects on cellular oxidant generation, which our investigators have previously shown to modulate autophosphorylation of the insulin receptor and its major postreceptor substrates upstream as well as downstream signaling through the activation of cellular glucose transport (34, 35). Furthermore, we and others have shown that an endogenous oxidant signal is integral to the cellular activation of Akt via the upstream stimulation of PI 3′-kinase (34, 43), which we have demonstrated in the present work is also attenuated by interference with Nox4 abundance or function.

The Nox4 deletion constructs lacking NAD(P)H or FAD/NAD(P)H cofactor binding domains appear to act in a dominant-negative fashion, inhibiting the generation of cellular H_2O_2 and insulin signaling, perhaps by interfering with coupling of the insulin receptor signal to endogenous Nox4. Besides the identification of a role for Nox4 as a component of the oxidant-generating system in 3T3-L1 cells reported here, little is known about additional components of this signaling complex that may have a regulatory role in insulin-sensitive cell types. The well-characterized NAD(P)H oxidase complex from phagocytic cells has a multisubunit structure, including plasma membrane and cytosolic components whose complex formation is highly regulated and tightly coupled to enzymatic superoxide production (1). Thus, overexpression of Nox4 with the deleted cofactor domains may inhibit the formation of a functional NAD(P)H oxidase complex in the 3T3-L1 system. A more detailed characterization of additional components of adipocyte Nox interaction proteins will help elucidate these regulatory mechanisms. Several groups have recently reported the cloning of Nox-interacting subunit proteins in nonphagocytic cells that have dramatic effects on the regulation of superoxide production by Nox1 (e.g., reference 4). These, or related proteins, may have a role in the regulation of Nox4 function in insulin and growth factor signaling. Also, small GTPases or heterotrimeric G-proteins may be involved in cellular oxidant production: rac has been shown to be a regulatory component of the phagocytic NAD(P)H oxidase complex (1), and evidence for the involvement of $G_{\alpha i2}$ in the adipocyte oxidant-generating system responsive to insulin has been reported (29).

Several cellular targets of H_2O_2 produced by growth factor stimulation have been identified, and our understanding of their role in signal transduction is beginning to unfold (24, 46). One of the major effects of oxidants that mimic insulin action involves the inhibition of thiol-dependent cellular enzymes, including PTPases, that modulate various steps in signal transduction from the insulin receptor (34, 35) as well as several other growth factor receptor-induced tyrosine phosphorylation cascades (31, 37). PTP1B is an intracellular PTPase that has been implicated in the regulation of insulin signaling in cellular and transgenic mouse studies (reviewed in references 18 and 44). Consistent with these reports, we found that PTP1B overexpression consistently reduces insulin-stimulated tyrosine phosphorylation of its receptor and IRS-1 (Fig. 5A to C). In addition, the effect of PTP1B on insulin signal transduction as well as the catalytic activity of PTP1B itself as isolated from the 3T3-L1 adipocytes following adenovirus-mediated gene delivery was markedly diminished by overexpression of Nox4 (Fig. 5C and 9). These results provide an important mechanistic link between the insulin-stimulated oxidant-generating machinery and PTP1B as a target of oxidative inhibition. Additional signaling molecules that are potential targets of oxidative inhibition via the Nox4 pathway are other key mediators of growth factor signaling, including, for example, the tyrosine phosphatase TCPTP (17) and the 3′-PI(3,4,5)-PO_4 phosphatase PTEN (32).

Further work will be needed to identify additional proteins that may have a role in the Nox4 signaling complex and to define the mechanism of coupling oxidant generation via Nox4 to the insulin receptor signaling cascade. This active area of research holds promise to define on a molecular basis a novel regulatory system for insulin action that was initially identified by observations made more than 30 years ago.

ACKNOWLEDGMENTS

We are grateful to Jonathan Chernoff (Fox Chase Cancer Center, Philadelphia, Pa.) for providing the original human PTP1B cDNAs and to John Flynn (Thomas Jefferson University) for the HADMEC cells used in these studies.

This work was supported by National Institutes of Health grant RO1 DK-43396 and a mentor-based postdoctoral fellowship grant from the American Diabetes Association to B. J. Goldstein. K. Mahadev is supported by a postdoctoral fellowship training grant award from the National Institute of Diabetes and Digestive and Kidney Diseases.

REFERENCES

1. **Babior, B. M., J. D. Lambeth, and W. Nauseef.** 2002. The neutrophil NADPH oxidase. Arch. Biochem. Biophys. **397:**342–344.
2. **Bae, Y. S., S. W. Kang, M. S. Seo, I. C. Baines, E. Tekle, P. B. Chock, and S. G. Rhee.** 1997. Epidermal growth factor (EGF)-induced generation of hydrogen peroxide. Role in EGF receptor-mediated tyrosine phosphorylation. J. Biol. Chem. **272:**217–221.
3. **Bae, Y. S., J. Y. Sung, O. S. Kim, Y. J. Kim, K. C. Hur, A. Kazlauskas, and S. G. Rhee.** 2000. Platelet-derived growth factor-induced H_2O_2 production requires the activation of phosphatidylinositol 3-kinase. J. Biol. Chem. **275:** 10527–10531.
4. **Banfi, B., R. A. Clark, K. Steger, and K. H. Krause.** 2003. Two novel proteins activate superoxide generation by the NADPH oxidase NOX1. J. Biol. Chem. **278:**3510–3513.
5. **Barrett, W. C., J. P. DeGnore, Y. F. Keng, Z. Y. Zhang, M. B. Yim, and P. B. Chock.** 1999. Roles of superoxide radical anion in signal transduction mediated by reversible regulation of protein-tyrosine phosphatase 1B. J. Biol. Chem. **274:**34543–34546.
6. **Bose, A., A. Guilherme, S. I. Robida, S. M. Nicoloro, Q. L. Zhou, Z. Y. Jiang, D. P. Pomerleau, and M. P. Czech.** 2002. Glucose transporter recycling in response to insulin is facilitated by myosin Myo1c. Nature **420:**821–824.
7. **Bradford, M. M.** 1976. A rapid and sensitive method for the quantitation of microgram quantities of protein utilizing the principle of protein-dye binding. Anal. Biochem. **72:**248–254.
8. **Cheng, G., Z. Cao, X. Xu, E. G. Van Meir, and J. D. Lambeth.** 2001. Homologs of gp91phox: cloning and tissue expression of Nox3, Nox4, and Nox5. Gene **269:**131–140.
9. **Cross, A. R., J. Rae, and J. T. Curnutte.** 1995. Cytochrome b-245 of the neutrophil superoxide-generating system contains two nonidentical hemes. Potentiometric studies of a mutant form of gp91phox. J. Biol. Chem. **270:** 17075–17077.
10. **Czech, M. P., J. C. Lawrence, Jr., and W. S. Lynn.** 1974. Evidence for electron transfer reactions involved in the Cu^{2+}- dependent thiol activation of fat cell glucose utilization. J Biol. Chem. **249:**1001–1006.
11. **Czech, M. P., J. C. Lawrence, Jr., and W. S. Lynn.** 1974. Evidence for the involvement of sulfhydryl oxidation in the regulation of fat cell hexose transport by insulin. Proc. Natl. Acad. Sci. USA **71:**4173–4177.
12. **Dadke, S., and J. Chernoff.** 2002. Interaction of protein tyrosine phosphatase (PTP) 1B with its substrates is influenced by two distinct binding domains. Biochem. J. **364:**377–383.
13. **Elchebly, M., P. Payette, E. Michaliszyn, W. Cromlish, S. Collins, A. L. Loy, D. Normandin, A. Cheng, J. Himms-Hagen, C. C. Chan, C. Ramachandran, M. J. Gresser, M. L. Tremblay, and B. P. Kennedy.** 1999. Increased insulin sensitivity and obesity resistance in mice lacking the protein tyrosine phosphatase-1B gene. Science **283:**1544–1548.
14. **Fingar, D. C., S. F. Hausdorff, J. Blenis, and M. J. Birnbaum.** 1993. Dissociation of pp70 ribosomal protein S6 kinase from insulin- stimulated glucose transport in 3T3-L1 adipocytes. J. Biol. Chem. **268:**3005–3008.
15. **Finkel, T.** 2000. Redox-dependent signal transduction. FEBS Lett. **476:**52–54.
16. **Flynn, J. T., M. Westbrooks, and K. A. Lucas.** 1997. Establishment and characterization of a line of adipose-derived human microvascular endothelial cells (HADMEC-5) transformed by simian virus 40 large T antigen expression: application to endotoxin research. Shock **8:**45–54.
17. **Galic, S., M. Klingler-Hoffmann, M. T. Fodero-Tavoletti, M. A. Puryer, T. C. Meng, N. K. Tonks, and T. Tiganis.** 2003. Regulation of insulin receptor signaling by the protein tyrosine phosphatase TCPTP. Mol. Cell. Biol. **23:** 2096–2108.
18. **Goldstein, B. J.** 2001. Protein-tyrosine phosphatase 1B (PTP1B): a novel therapeutic target for type 2 diabetes mellitus, obesity and related states of insulin resistance. Curr. Drug Targets Immune Endocr. Metabol. Disorders **1:**265–275.
19. **Goldstein, B. J.** 2002. Protein-tyrosine phosphatases: emerging targets for therapeutic intervention in type 2 diabetes and related states of insulin resistance. J. Clin. Endocrinol. Metab. **87:**2474–2480.
20. **Griendling, K. K., and M. Ushio-Fukai.** 2000. Reactive oxygen species as mediators of angiotensin II signaling. Regul. Peptides **91:**21–27.
21. **Herrlich, P., and F. D. Bohmer.** 2000. Redox regulation of signal transduction in mammalian cells. Biochem. Pharmacol. **59:**35–41.
22. **Junn, E., K. N. Lee, H. R. Ju, S. H. Han, J. Y. Im, H. S. Kang, T. H. Lee, Y. S. Bae, K. S. Ha, Z. W. Lee, S. G. Rhee, and I. Choi.** 2000. Requirement of hydrogen peroxide generation in TGF-beta 1 signal transduction in human lung fibroblast cells: involvement of hydrogen peroxide and Ca^{2+} in TGF-beta 1-induced IL-6 expression. J. Immunol. **165:**2190–2197.
23. **Kido, Y., J. Nakae, and D. Accili.** 2001. The insulin receptor and its cellular targets. J. Clin. Endocrinol. Metab. **86:**972–979.
24. **Kim, J. R., H. W. Yoon, K. S. Kwon, S. R. Lee, and S. G. Rhee.** 2000. Identification of proteins containing cysteine residues that are sensitive to oxidation by hydrogen peroxide at neutral pH. Anal. Biochem. **283:**214–221.
25. **Klaman, L. D., O. Boss, O. D. Peroni, J. K. Kim, J. L. Martino, J. M. Zabolotny, N. Moghal, M. Lubkin, Y. B. Kim, A. H. Sharpe, A. Stricker-Krongrad, G. I. Shulman, B. G. Neel, and B. B. Kahn.** 2000. Increased energy expenditure, decreased adiposity, and tissue-specific insulin sensitivity in protein-tyrosine phosphatase 1B-deficient mice. Mol. Cell. Biol. **20:** 5479–5489.
26. **Krieger-Brauer, H. I., and H. Kather.** 1992. Human fat cells possess a plasma membrane-bound H_2O_2-generating system that is activated by insulin via a mechanism bypassing the receptor kinase. J. Clin. Investig. **89:**1006–1013.
27. **Krieger-Brauer, H. I., and H. Kather.** 1995. Antagonistic effects of different members of the fibroblast and platelet-derived growth factor families on adipose conversion and NADPH-dependent H_2O_2 generation in 3T3-L1 cells. Biochem. J. **307:**549–556.
28. **Krieger-Brauer, H. I., and H. Kather.** 1995. The stimulus-sensitive H_2O_2-generating system present in human fat-cell plasma membranes is multireceptor-linked and under antagonistic control by hormones and cytokines. Biochem. J. **307:**543–548.
29. **Krieger-Brauer, H. I., P. K. Medda, and H. Kather.** 1997. Insulin-induced activation of NADPH-dependent H_2O_2 generation in human adipocyte plasma membranes is mediated by $G_{\alpha i2}$. J. Biol. Chem. **272:**10135–10143.
30. **Lambeth, J. D.** 2002. Nox/Duox family of nicotinamide adenine dinucleotide (phosphate) oxidases. Curr. Opin. Hematol. **9:**11–17.
31. **Lee, S. R., K. S. Kwon, S. R. Kim, and S. G. Rhee.** 1998. Reversible inactivation of protein-tyrosine phosphatase 1b in A431 cells stimulated with epidermal growth factor. J. Biol. Chem. **273:**15366–15372.
32. **Lee, S. R., K. S. Yang, J. Kwon, C. Lee, W. Jeong, and S. G. Rhee.** 2002. Reversible inactivation of the tumor suppressor PTEN by H_2O_2. J. Biol. Chem. **277:**20336–20342.
33. **Livingston, J. N., P. A. Gurny, and D. H. Lockwood.** 1977. Insulin-like effects of polyamines in fat cells. Mediation by H_2O_2 formation. J. Biol. Chem. **252:**560–562.
34. **Mahadev, K., X. Wu, A. Zilbering, L. Zhu, J. T. R. Lawrence, and B. J. Goldstein.** 2001. Hydrogen peroxide generated during cellular insulin stimulation is integral to activation of the distal insulin signaling cascade in 3T3-L1 adipocytes. J. Biol. Chem. **276:**48662–48669.
35. **Mahadev, K., A. Zilbering, L. Zhu, and B. J. Goldstein.** 2001. Insulin-stimulated hydrogen peroxide reversibly inhibits protein-tyrosine phosphatase 1B in vivo and enhances the early insulin action cascade. J. Biol. Chem. **276:**21938–21942.
36. **May, J. M., and C. de Haen.** 1979. Insulin-stimulated intracellular hydrogen peroxide production in rat epididymal fat cells. J. Biol. Chem. **254:**2214–2220.
37. **Meng, T. C., T. Fukada, and N. K. Tonks.** 2002. Reversible oxidation and inactivation of protein tyrosine phosphatases in vivo. Mol. Cell **9:**387–399.
38. **Mukherjee, S. P., and W. S. Lynn.** 1977. Reduced nicotinamide adenine dinucleotide phosphate oxidase in adipocyte plasma membrane and its activation by insulin. Possible role in the hormone's effects on adenylate cyclase and the hexose monophosphate shunt. Arch. Biochem. Biophys. **184:**69–76.
39. **Nisimoto, Y., H. Otsuka-Murakami, and D. J. Lambeth.** 1995. Reconstitution of flavin-depleted neutrophil flavocytochrome b_{558} with 8-mercapto-FAD and characterization of the flavin-reconstituted enzyme. J. Biol. Chem. **270:**16428–16434.
40. **Orlicky, D. J., and J. Schaack.** 2001. Adenovirus transduction of 3T3-L1 cells. J. Lipid Res. **42:**460–466.
41. **Rhee, S. G., Y. S. Bae, S. R. Lee, and J. Kwon.** 2000. Hydrogen peroxide: a key messenger that modulates protein phosphorylation through cysteine oxidation. Sci. STKE **2000:**E1.
42. **Saltiel, A. R., and C. R. Kahn.** 2001. Insulin signalling and the regulation of glucose and lipid metabolism. Nature **414:**799–806.
43. **Shaw, M., P. Cohen, and D. R. Alessi.** 1998. The activation of protein kinase B by H_2O_2 or heat shock is mediated by phosphoinositide 3-kinase and not by mitogen-activated protein kinase-activated protein kinase-2. Biochem. J. **336:**241–246.
44. **Tonks, N. K.** 2003. PTP1B: from the sidelines to the front lines! FEBS Lett. **546:**140–148.
45. **White, M. F.** 2002. IRS proteins and the common path to diabetes. Am. J. Physiol. Endocrinol. Metab. **283:**E413–E422.
46. **Woo, H. A., H. Z. Chae, S. C. Hwang, K. S. Yang, S. W. Kang, K. Kim, and S. G. Rhee.** 2003. Reversing the inactivation of peroxiredoxins caused by cysteine sulfinic acid formation. Science **300:**653–656.
47. **Zhu, L., A. Zilbering, X. Wu, K. Mahadev, J. I. Joseph, S. Jabbour, W. Deeb, and B. J. Goldstein.** 2001. Use of an anaerobic environment to preserve the endogenous activity of protein-tyrosine phosphatases isolated from intact cells. FASEB J. **15:**1637–1639.